Some Physical Properties Improvement Nickel Oxide Thin Films with Cadmium doping

Abeer Ghalib Hadi

Ministry of Education/ General Directorate of Education in Baghdad Governorate/ Rusafa second, Iraq.

Abstract:

undoped NiO and NiO: Cd films were deposited by chemical spray pyrolysis (CSP). The color of NiO thin films were black-grey which is related to the nonstoichiometry of the deposited material. The crystal structure of the NiO thin films were cubic face centered and polycrystalline as specified by XRD patterns. The XRD peaks along (111), (200) and (220) planes showed highest intensity correspond to the preferred orientation (111) for NiO films at 3% Cadmium. The variation of grain sizes is found to be between 75.85 and 62.09 nm, whereas the strain increased from 27.30 to 30.19. NiO thin films is found to be smooth and homogenous by using atomic force microscopy (AFM). UV-Visible spectrophotometer is used to study the spectral transmittance of the films for wavelengths between 300 to 900 nm. Increasing doping concentration of Cadmium lead to decrease in the transmittance values. However, increasing Cd concentration cause increasing the absorption coefficient values. Furthermore, increasing the band gap from 3.60 to 3.69eV is related to increasing Cadmium doping ratio. Whereas, the extinction coefficient and refractive index decreased when Cadmium doping ratio is increased.

Keywords: (NiO, thin films, CSP, Structural, Optical Properties).

بعض الخصائص الفيزيائية تحسن النيكل
أغشية أكسيد رقيقة مع منشطات الكاديوم

عبير غالب هادي
وزارة التربية / المديرية العامة للتربية في محافظة بغداد / الرصافة الثانية العراق.

الملخص:

NiO و NiO غير المغسولة: ترسبت أغشية الكاديوم عن طريق الانحلال الحراري بالرش الكيميائي .(CSP) كان لون أغشية NiO الرقيقة أسود-رمادي وهو مرتبط بقياس عدم التكافؤ للمادة المترسبة. كان التركيب البلوري لأغشية NiO الرقيقة متمركزًا على وجه مكعب ومتعدد البلورات كما هو محدد بواسطة أنماط .XRD أظهرت قمم XRD على طول (١١١) و (٢٠٠) و (٢٢٠)

أعلى كثافة تتوافق مع الاتجاه المفضل (١١١) لأفلام NiO بنسبة ٣ ٪ كادميوم. تم العثور على تباين أحجام الحبوب بين ٧٥.٨٥ و ٦٢.٠٩ نانومتر ، بينما زاد الضغط من ٢٧.٣٠ إلى ٣٠.١٩. تم العثور على أغشية NiO الرقيقة لتكون ناعمة ومتجانسة باستخدام مجهر القوة الذرية .(AFM) يستخدم مقياس الطيف الضوئي المرئي فوق البنفسجي لدراسة النفاذية الطيفية للأغشية لأطوال موجية بين ٣٠٠ إلى ٩٠٠ نانومتر. تؤدي زيادة تركيز المنشطات للكادميوم إلى انخفاض قيم النفاذية. ومع ذلك ، فإن زيادة تركيز الكادميوم يؤدي إلى زيادة قيم معامل الامتصاص. علاوة على ذلك ، فإن زيادة فجوة النطاق من ٣.٦٠ إلى ٣.٦٩ eV مرتبطة بزيادة نسبة المنشطات للكادميوم. في حين انخفض معامل الانقراض ومعامل الانكسار عند زيادة نسبة تعاطي الكادميوم.

الكلمات المفتاحية :(NiO ، الأغشية الرقيقة ، CSP، الإنشائية ، الخواص البصرية).

Introduction

NiO is part of TCO family that has several advantages such as good adsorptive properties and chemical stability. NiO is suitable to be deposited on several types of substrates such as glass, ceramics, or oxides [1,2]. The oxides metallic that has semiconductor behavior can be utilized in various applications for example gas sensors, photocatalysis, optoelectronics, lithium-ion micro batteries, and many others [2–14]. NiO exhibited direct band gap ranging from 3.6-4.0 eV as reported by literature [15, 16]. There are several techniques to synthesize NiO thin layers, such as CVD [17], sol-gel process [18], electron-beam evaporation [19], PLD [20], dc-magnetron sputtering [21], spray pyrolysis [22], atomic layer deposition (ALD) [23], electrodeposition process [24] and the chemical bath deposition (CBD) [25]. spray pyrolysis method is an appropriate method due to many important advantages such as the deposition area can be large compared with other deposition techniques, unexpensive, high vacuum is not required, [22]. According to the mentioned advantages, a thin film of Undoped NiO and NiO: Cd were deposit via CSP. In this work, some physical properties of the Undoped NiO and NiO: Cd are carried out to study the effect of adding Cadmium as a dopant.

Experimental

The samples of Cd-doped NiO thin films are prepared using CSP. To prepare a 0.1 M coating solution, dissolve ($NiCl_2.6H_2O$) in 100 ml of redistilled water. Cadmium has a volumetric ratio of 1.3 percent. The substrate was heated to 400 degrees Celsius. The layers were placed onto

glass substrates that had previously been chemically and ultrasonically cleaned. Spraying rate 0.2 ml/spray, base to spout 29 cm, spraying time 8 sec, the period between successive sprays 2 min, and the transporter gas (air) was preserved at a pressure of 10^5 Pa were all taken into account to optimize the deposition. To measure thickness, the gravimetric method is applied. and found to be around 300 nm. X-ray diffractometer used to study structural properties. AFM was used to investigate the surface of the films. Optical transmittance spectra were studied using UV-Visible spectrophotometer.

Results and Discussions

XRD styles of the intended films are presented in Figure (1). XRD exhibited peaks around (2θ~37.10^o, 43.32^o and 62.83^o) assigned to (111), (200) and (220) respectively. These results were in covenant with ICDD card number 04-0835. The maximum peak found to be at 2θ~37.10^o which assigned to (111) plane. The peaks values and the occurrence of multiple peaks means the prepared thin film were polycrystalline and has cubic structure which is covenant with the reported experimental results [26, 27].

The grain size of the crystallite (D) of the intended films are calculated from the XRD data using the Scherrer formula [28]:

$$D = \frac{k\,\lambda}{\beta cos\theta} \qquad (1)$$

Where λ is the x-ray wavelength used, k = 0.9 and θ is Bragg's angle.

By increasing Cadmium doping concentration from 1% to 3%, *D* of the undoped NiO thin films increased and reached its highest value 12.69 nm, see Figure 2.

The dislocation density (δ) is gained by the following Eq. [29]:

$$\delta = \frac{1}{D^2} \qquad (2)$$

Dislocation density (δ) decreased from 75.85 to 62.09, see Table 1.

To calculate the strain (ε) the following formula is used [30]:

$$\varepsilon = \frac{\beta cos\theta}{4} \qquad (3)$$

Table 1. showed that strain (ε) decreased from 30.19 to 27.30. Structural parameters S_c were shown in Figure (2).

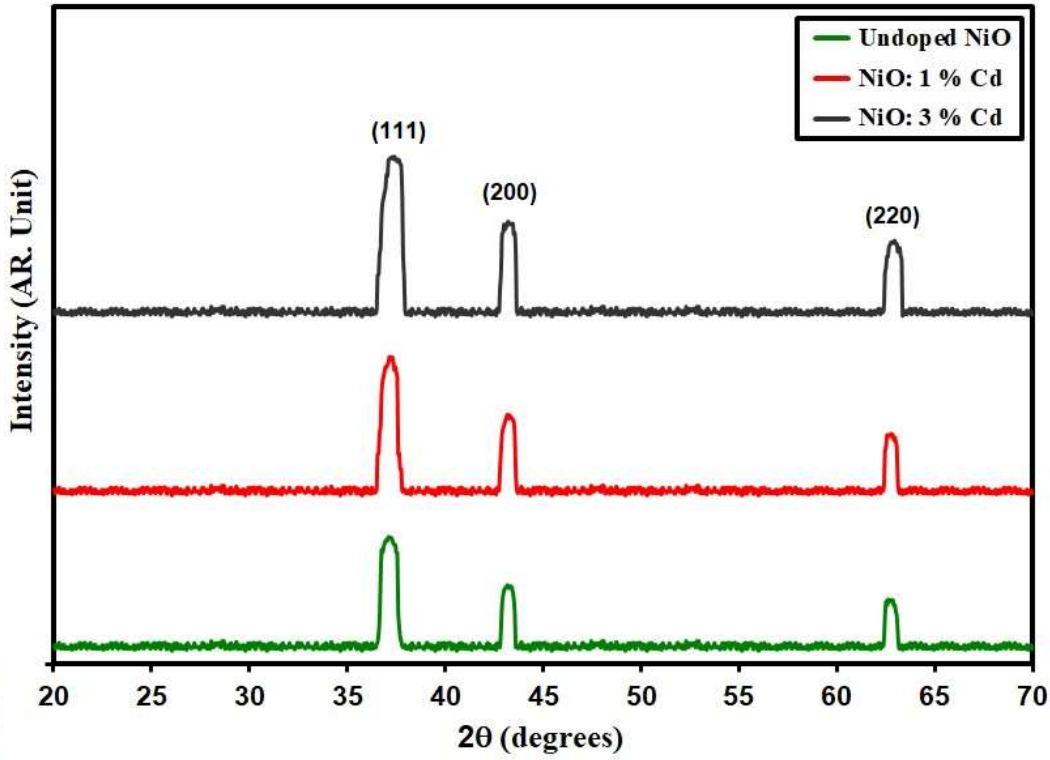

Fig.1. XRD styles of grown films.

Table 1. *D*, optical bandgap and Sc of grown films.

Sample	2 θ (^{o})	(hkl) Plane	FWHM (^{o})	E_g (eV)	*D* (nm)	δ ($\times 10^{14}$) (lines/m^2)	Strain ($\times 10^{-4}$)
Undoped NiO	37.10	111	0.73	3.69	11.48	75.85	30.19
NiO: 1% Cd	37.08	111	0.70	3.65	11.97	69.79	28.95
NiO: 3% Cd	37.05	111	0.66	3.60	12.69	62.09	27.30

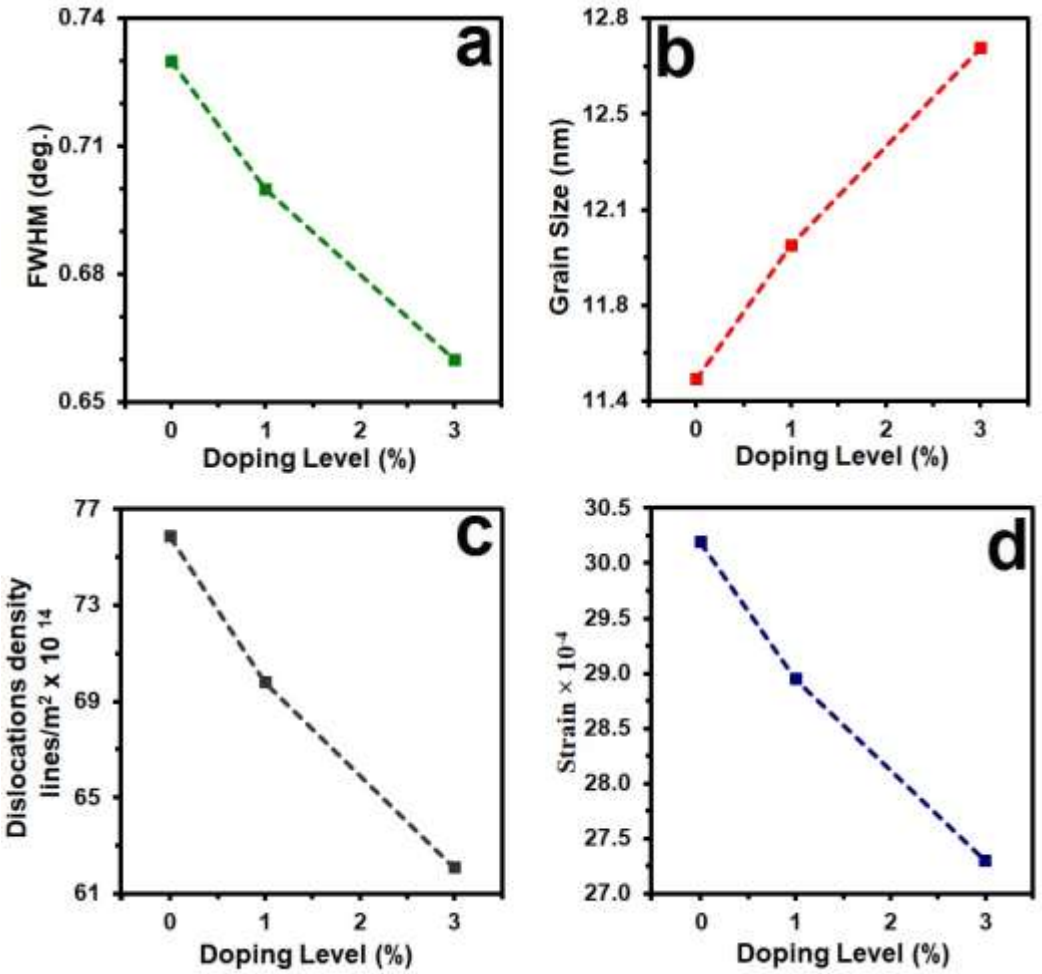

Fig.2. Sc of the grown films.

The 3D AFM micrographs are presented in Figure (3). The images exhibit homogenous and fine NiO thin films. The average Particle size P_{av} decreased from 78.39 nm to 64.73 nm by increasing for undoped NiO and NiO: 3% Cd. From Figure 3 (a_3, b_3 and c_3). The surface roughness and rms values were (8.05, 4.75 and 3.63) nm and 7.63, 5.63 and 3.97) nm as Cd content increase. Table (2) offers AFM parameters A_P.

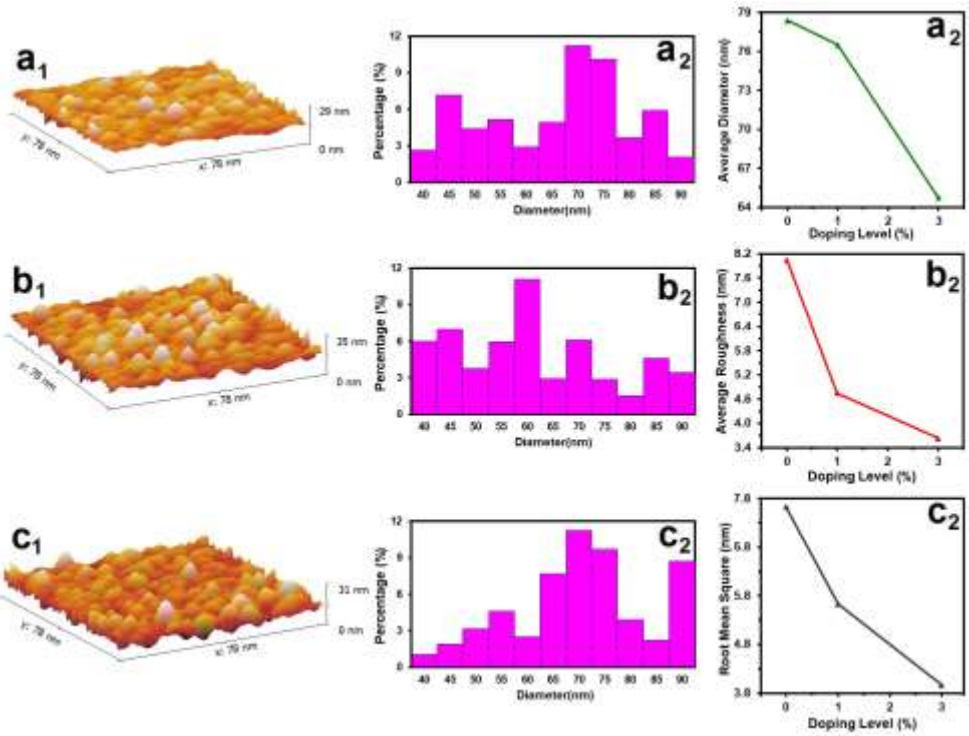

Fig.3. AFM images (a_1, b_1 and c_1), granularly distributed (a_2, b_2 and c_2) and diversity of A_P

Table 2. A_P of the intended films.

Samples	P_{av} nm	R_a (nm)	R. M. S. (nm)
Undoped NiO	78.39	8.05	7.63
NiO: 1% Cd	76.49	4.75	5.63
NiO: 3% Cd	64.73	3.63	3.97

Figure (5) represents the optical transmission(T) via wavelength. One can notice that the optical transmission is decreasing with increasing the concentration of Cadmium doping [31].

The absorption coefficient (α) determines the ability of a material that can absorb a specific spectrum. Using the equation [32]:

$$\alpha = \ln (1/T)/d \qquad (4)$$

Where, d is film thickness.

Fig.5 displays absorption coefficient (α) decreased with an increase at 1% or 3 % Cadmium doping.

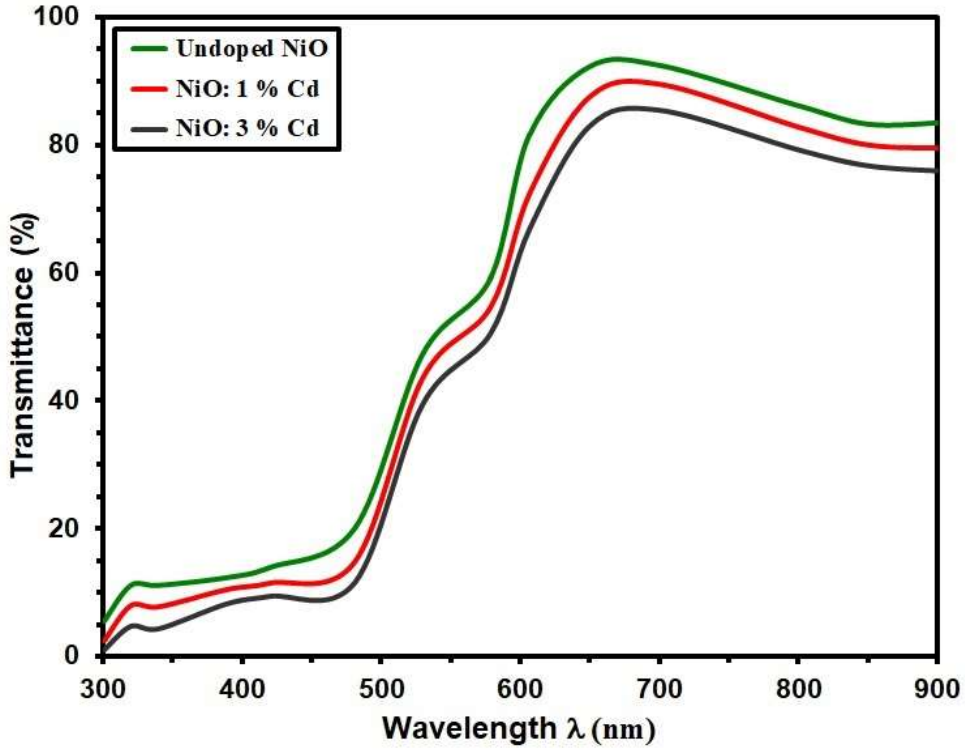

Fig. 4: T with wavelength of grown films.

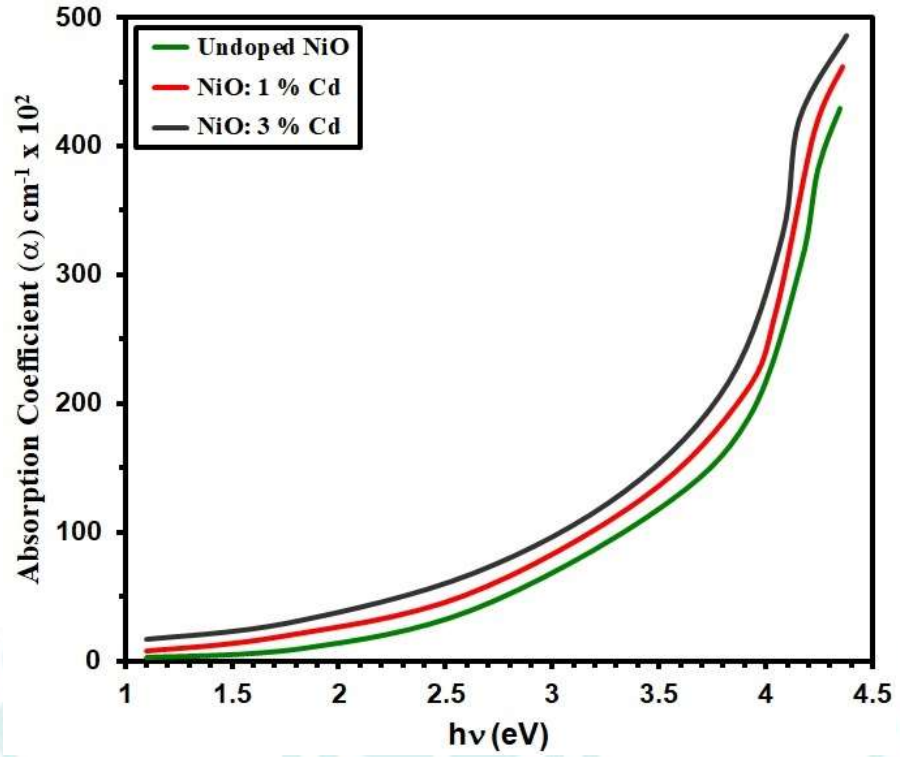

Fig. 5: α via hν of intended films.

The bandgap E_g is determined by Tauc 's equations [33]:

$$(\alpha h\nu) = A\left(h\nu - E_g\right)^{\frac{1}{2}} \qquad (5)$$

Where A is the constant, $(\alpha h\upsilon)^2$ against incident photon energy ($h\upsilon$), plots were gained.

as offers in Fig. (6) E_g shows a decrement with Cd-doping from 3.69 eV to 3.60 eV as Cd content increase.

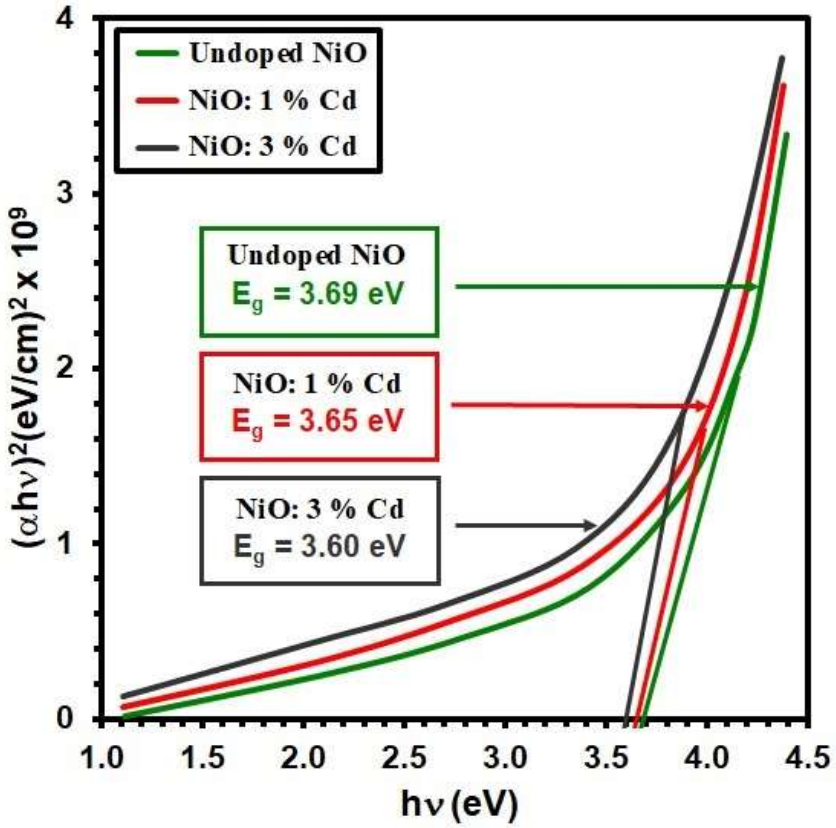

Fig. 6: $(\alpha h\nu)^2$ via hν of intended films.

The extinction coefficient (k) is obtained from the equation [34]:

$$k = \frac{\alpha\lambda}{4\pi} \quad \text{-----(6)}$$

Where α is the absorption coefficient. *K* are plotted in Fig.7 for NiO: 4% Cd thin films. The extinction coefficient decreased with increasing Cadmium doping concentration increase.

Refractive index (n) is determined using the following equation [35]:

$$n = \left(\frac{1+R}{1-R}\right) + \sqrt{\frac{4R}{(1-R)^2} - k^2} \quad \text{----- (7)}$$

Where R is the reflectance.

Fig. 8 represent refractive index with wavelength, and it's clear from this figure the refractive index increased with wavelength until 540 nm and with

the Cadmium doping, and then decreased at wavelength greater than 540 nm and with increasing Cadmium doping, there is a little decrease in n via Cadmium doping.

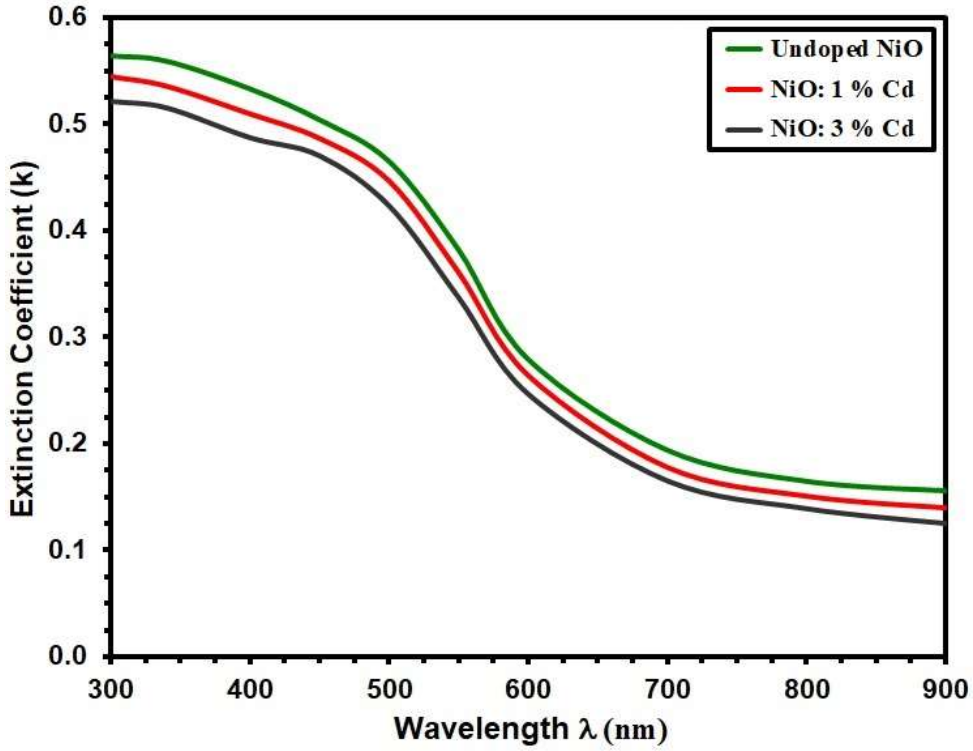

Fig. 7: k of intended films.

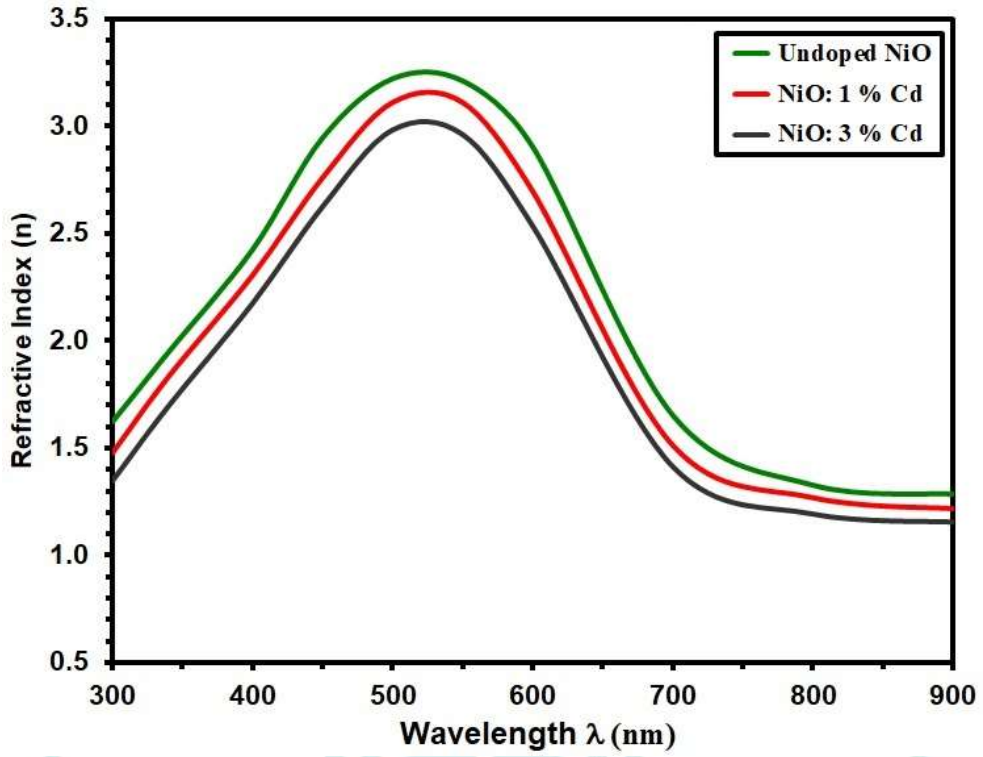

Fig. 8. n of intended films.

Conclusion

The CSP is used to deposit nickel oxide Thin film. The peaks values of X-ray diffraction (XRD) show polycrystalline and cubic crystalline with a predominant orientation along (111). AFM image exhibits the variation of grain size where it is 78.39 nm and 64.73 nm for undoped NiO and NiO:3% Cd, respectively. In the visible light region, the average transmission is found to be 95% and the band gap ranging from 3.69 and 3.60 eV. The absorption coefficient is increased by increasing the dopant concentration. However, the extinction coefficient and the refractive index showed an opposite behavior where their values are decreased with increasing dopant concentration.

References

[1] Gund G.S., Lokhande C.D., Park H.S., Controlled synthesis of hierarchical nanoflake structure of NiO thin film for supercapacitor application, Journal of Alloys and Compounds 741 (2018) 549-556.
[2] Aoun Y., Meneceur R., Benramache S., Maaoui B., Sprayed NiO-Doped p-Type Transparent ZnO Thin Films Suitable for Gas-Sensing Devices, Physics of the Solid State 62 (1) (2020) 131–136.
[3] Raza M.H., Movlaee K., Wu Y., El- Refaei S.M., Karg M., Leonardi S.G., Neri G., Pinna N., Tuning the NiO Thin Film Morphology on Carbon Nanotubes by Atomic Layer Deposition for Enzyme- Free Glucose Sensing, ChemElectroChem 6 (2019) 383–392.
[4] Herissi L., Hadjeris L., Aida M.S., Bougdira J., Properties of (NiO) 1-x (ZnO) x thin films deposited by spray pyrolysis, Thin Solid Films 605 (2016) 116–120.
[5] Guezzoun H., Benhaoua B., Benramache S., Synthesis and characterizations of nanocrystalline Na and Al codoped NiO thin films, International Journal of Integrated Engineering 12 (1) (2020) 204-209.
[6] R. O. Ijeh *et al.*, "Magnetic and optical properties of electrodeposited nanospherical copper doped nickel oxide thin films," *Physica E: Low-dimensional Systems and Nanostructures*, vol. 113, pp. 233–239, Sep. 2019,
[7] A. J. Haider, R. Al- Anbari, H. M. Sami, and M. J. Haider, "Photocatalytic Activity of Nickel Oxide," *Journal of Materials Research and Technology*,
[8] Jung, D. L. Kim, S. H. Oh, and H. J. Kim, "Stability enhancement of organic solar cells with solution-processed nickel oxide thin films as hole transport layers," *Solar Energy Materials and Solar Cells*, vol. 102, pp. 103–108, Jul. 2012.
[9] M. Napari *et al.*, "Antiferromagnetism and p-type conductivity of nonstoichiometric nickel oxide thin films," *InfoMat*, vol. 2, no. 4, pp. 769–774, 2020.
[10] A. M. Soleimanpour, A. H. Jayatissa, and G. umanasekera, "Surface and gas sensing properties of nanocrystalline nickel oxide thin films," *Applied Surface Science*, vol. 276, pp. 291–297, Jul. 2013.
[11] G. S. Gund, C. D. Lokhande, and H. S. Park, "Controlled synthesis of hierarchical nanoflake structure of NiO thin film for

supercapacitor application," *Journal of Alloys and Compounds*, vol. 741, pp. 549–556, Apr. 2018.

[12] H. Lin *et al.*, "The growth, properties and application of reactively sputtered nickel oxide thin films in all thin film electrochromic devices," *Materials Science and Engineering: B*, vol. 270, p. 115196, Aug. 2021.

[13] S. J. Lee, T.-G. Lee, S. Nahm, D. H. Kim, D. J. Yang, and S. H. Han, "Investigation of all-solid-state electrochromic devices with durability enhanced
tungsten-doped nickel oxide as a counter electrode," *Journal of Alloys and Compounds*, vol. 815, p. 152399, Jan. 2020.

[14] H. Yang, J.-H. Yu, H. J. Seo, R. H. Jeong, and J.-H. Boo, "Improved electrochromic properties of nanoporous NiO film by NiO flake with thickness
controlled by aluminum," *Applied Surface Science*, vol. 461, pp. 88–92, Dec. 2018.

[15] Shang Z.W., Hsu H.H., Zheng Z.W., Cheng C.H., Progress and challenges in p-type oxide-based thin film transistors, Nanotechnology Reviews 8 (2019) 422–443.

[16] Hotovy I., Spiess L., Predanocy M., Rehacek V., Racko J., Sputtered nanocrystalline NiO thin films for very low ethanol detection, Vacuum 107 (2014) 129–131.

[17] A. S. Kondrateva, M. V. Mishin, and S. E.Alexandrov, "TOF MS Investigation of Nickel Oxide CVD," *J. Am. Soc. Mass Spectrom.*, vol. 28, no. 11, pp. 2352–2360, Nov. 2017.

[18] S. Zargouni, S. El Whibi, E. Tessarolo, M. Rigon, A. Martucci, and H. Ezzaouia, "Structural properties and defect related luminescence of Yb-doped NiO sol-gel thin films," *Superlattices and Microstructures*, vol. 138, p. 106361, Feb. 2020.

[19] D. R. Sahu, T.-J. Wu, S.-C. Wang, and J.-L. Huang, "Electrochromic behavior of NiO film prepared by e-beam evaporation," *Journal of Science: Advanced Materials and Devices*, vol. 2, no. 2, pp. 225–232.

[20] M. A. Hameed, O. A. Ali, and S. S. M. Al-Awadi, "Optical properties of Ag-doped nickel oxide thin films prepared by pulsed-laser deposition technique," *Optik*, vol. 206, p. 164352, Mar. 2020.

[21] P. Salunkhe, M. A. A.V, and D. Kekuda, “Structural, spectroscopic and electrical properties of dc magnetron sputtered NiO thin films and an insight into
different defect states,” *Appl. Phys. A*, vol. 127, no. 5, p. 390, Apr. 2021.
[22] K. O. Ukoba, A. C. Eloka-Eboka, and F. L. Inambao, “Review of nanostructured NiO thin film deposition using the spray pyrolysis technique,” *Renewable and Sustainable Energy Reviews*, vol. 82, pp. 2900–2915, Feb. 2018.
[23] M. H. Raza *et al.*, “Tuning the NiO Thin Film Morphology on Carbon Nanotubes by Atomic Layer Deposition for Enzyme-Free Glucose Sensing,” *ChemElectroChem*, vol. 6, no. 2, pp. 383–392, 2019.
[24] B. R. Cruz-Ortiz, M. A. Garcia-Lobato, E. R. Larios-Duran, E. M. Muzquiz-Ramos, and J. C. Ballesteros-Pacheco, “Potentiostatic electrodeposition of nanostructured NiO thin films for their application as electrocatalyst,” *Journal of Electroanalytical Chemistry*, vol. 772, pp. 38–45, Jul. 2016.
[25] J.-H. Yu, S.-H. Nam, Y. E. Gil, and J.-H. Boo, “The effect of ammonia concentration on the microstructure and electrochemical properties of NiO nanoflakes array prepared by chemical bath deposition,” *Applied Surface Science*, vol. 532, p. 147441, Dec. 2020.
26] IsmailR. A., S.Ghafori, G. A. Kadhim, "Preparation and characterization of nanostructurednickel oxide thin films by spray pyrolysis",*Appl.Nanosci.,*vol. 3,pp. 509-514, 2013.
[27] BaluA.R., V.S.Nagarethinam, N. Arunkumar, M. Suganya, "NanocrystallineNiOthinfilms prepared by a low cost simplified spray technique usingperfume atomizer", *Journal of Electron Devices,*vol.13,pp.920-930, 2012.
[28] Garcia-Garcia F.J., Salazar P., Yubero F., González-Elipe A.R., Non-enzymatic glucose electrochemical sensor made of porous NiO thin films prepared by reactive magnetron sputtering at oblique angles, Electrochimica Acta 201 (2016) 38–44.
[29] Mironova-Ulmane N., Kuzmin A., Sildos I., Puust L., Grabis J., Magnon and Phonon Excitations in Nanosized NiO, Latvian Journal of Physics and Technical Sciences 56 (2019) 726–737.
[30] Manouchehri I., Mehrparvar D., Moradiana R., Gholami K., Osati T., Investigation of structural and optical properties of copper doped NiO thin

films deposited by RF magnetron reactive sputtering, Optik 127 (2016) 8124–8129.

[31] H. Lee, Y.-T. Huang, M. W. Horn, and S.-P. Feng, “Engineered optical and electrical performance of rf– sputtered undoped nickel oxide thin films for inverted perovskite solar cells,” *Sci Rep*, vol. 8, no. 1, p. 5590, Apr. 2018,

[32] R. Paulose, R. Mohan, and V. Parihar, “Nanostructured nickel oxide and its electrochemical behaviour—A brief review,” *Nano-Structures & Nano-Objects*, vol. 11, pp. 102–111, Jul. 2017,

[33] E. Fujii, A. Tomozawa, H. Torii, R. Takayama, “Preferred orientations of NiO films prepared by plasma-enhanced metalorganicchemical vapor deposition”,Jpn. J. Appl. Phys35(1996) L328–L330.

[34] K. Yoshimura, T. Miki, S. Tanemura, “Nickel oxide electrochromic thin films prepared by reactive DC magnetron sputtering”, Jpn. J. Appl. Phys.34(1995) 2440–2446.

[34] I. Hotovy, V. Rehacek, P. Siciliano, S. Capone, L. Spiess, “Sensing characteristics of NiO thin films as NO_2 gas sensor”,Thin Solid Films 418 (2002) 9–15.